Joint Pathology Center
Veterinary Pathology Services

WEDNESDAY SLIDE CONFERENCE 2025-2026

Conference #6 — 1 October 2025

CASE I:

Signalment:
Two year and nine month-old, male castrated, mixed breed, canine
Three year-old, male intact, Golden retriever, canine
Eight year-old, male castrated, mixed breed, canine
Fifteen year-old, male castrated, Labrador, canine

History:
Acute onset of vomiting and collapse.

Gross Pathology:
Segmental hemorrhagic necrosis of the bowel with perforation and peritonitis

Laboratory Results:
N/A

Microscopic Description:
Findings are very similar in all cases that were submitted to the diagnostic laboratory.

In all samples from the grossly discolored and swollen segment there was transmural necrosis of the intestine with extensive hemorrhage extending into the mesenteric fat. In the adjacent viable intestine there was eosinophilic infiltration of variable intensity. There was multifocal necrosis of mesenteric fat and, in some sections, diffuse eosinophilic infiltration.

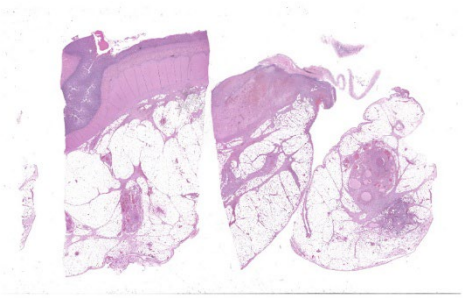

Figure 1-1: Intestine and mesentery. Three sections of intestine and mesentery are submitted for examination. At this magnification, the vessels of the mesentery and septa between lobules of mesenteric fat is expanded in each section. (HE, 10X)

Large vessels were dilated and many contained thrombi.

Within the media of medium to small sized arteries there were sections (not present in all slides due to the small size of the parasite – but see photomicrographs) of a nematode larva, approximately 100-200 µm in diameter with lateral allae and central digestive tract. These features are consistent with a spirurid of which *Spirocerca* is the most likely in our region. Foci of necrosis with hemorrhage were observed in the media of some arteries, where no larvae were identified.

Contributor's Morphologic Diagnoses:
Acute transmural necrotizing eosinophilic enteritis and eosinophilic peritonitis with arterial mesenteric thrombi and rare intralesional nematode larvae (spirurid)

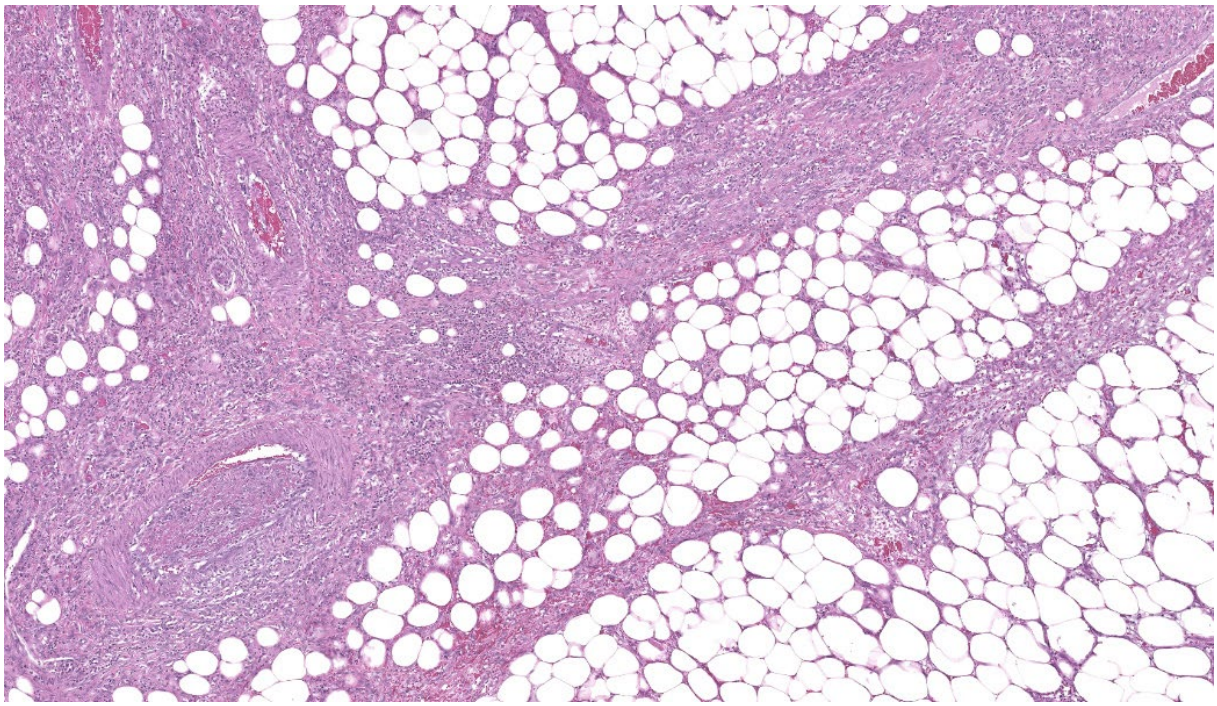

Figure 1-2: Mesentery, dog. Granulation tissue and eosinophilic inflammation expand the interlobular septa between lobules of mesenteric fat. A recanalized arteriole is present at bottom left. (HE, 80X)

Contributor's Comment:

Several cases of this condition were diagnosed in the last few years in Israel, where incidence of *Spirocerca* infection is high.[1,7] We have not observed breed or age predilection. The presenting history is usually that of intestinal infarction, with or without peritonitis. Clinical DDs are volvulus or intussusception.

Heavy eosinophilic infiltration of mesenteric fat and thrombi are a common histologic finding in all samples in addition to acute transmural intestinal necrosis. In only a few of the samples intralesional larvae have been observed.

Some samples with similar history which were received in the past, before we became aware of this condition, were evaluated retrospectively. Although no parasites were found, we considered the presence of heavy eosinophilic infiltration and thrombi to be highly suggestive of aberrant larval migration of *Spirocerca*.

Follow up information was available for some of these dogs. The vets described recurrent intestinal infarction and peritonitis with or without perforation.

Spirocerca lupi is a spirurid nematode that parasitizes the esophageal wall of dogs and

Figure 1-3: Mesentery, dog. A tangential section of a larval nematode is present in he wall of a mesenteric artery. (HE, 100X) (Photo courtesy of: The Weizmann Institute of Science, http://www.weizmann.ac.il/)

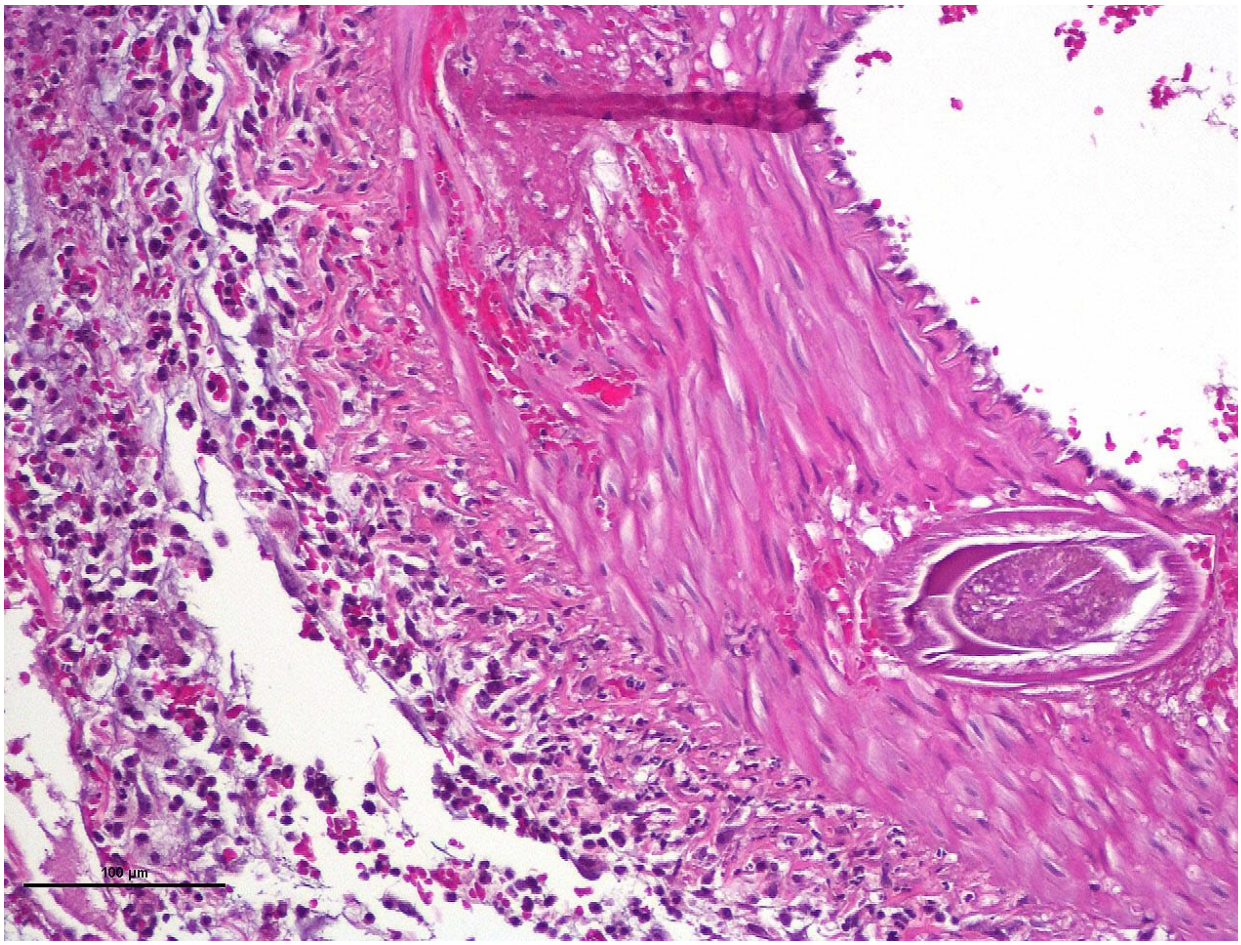

Figure 1-4: Mesentery, dog. Higher magnification of a tangential section of a larval nematode within the wall of a mesenteric artery. (HE, 400X) (Photo courtesy of: The Weizmann Institute of Science, http://www.weizmann.ac.il/)

other carnivores. It is most common in warm climates where beetles act as intermediate hosts.[1,2,7] The normal site for the adult nematode is the distal region of the esophageal submucosa or the proximal stomach, where they are found in a cystic granulomatous lesion.[2]

Third stage larvae of *Spirocerca* are ingested with beetles and penetrate the gastric mucosa. They move along arteries to the aorta and migrate in its wall to the thoracic region where they are found several weeks after ingestion. They incite granulomatous inflammation in the aorta and stay there for 2-4 months. Later, the larvae migrate to the esophagus where they mature in the submucosa and perforate the epithelium.[2,7]

Larvae that follow aberrant migratory pathways may be found in granulomas in subcutaneous tissue, bladder, kidney, spinal cord and intrathoracic locations.[2,3,9] To our knowledge, there are no descriptions of Spirocerca in mesenteric blood vessels.

Aortic lesions associated with *Spirocerca* include intimal and medial hemorrhage and necrosis with eosinophilic inflammation, thrombus formation and rarely rupture of the aortic wall.[1,2,7]

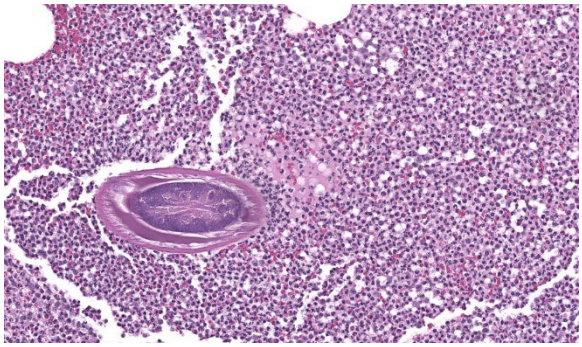

Figure 1-5: Mesentery, dog. A tangential section of a larval nematode in an area of eosinophilic inflammation demonstrates a smooth cuticle, polymyarian-coelomyarian musculature, a pseudocoelom containing bright red material (characteristic of spirurids) and and a single cross section of a large intestine. (HE, 800X) (*Photo courtesy of:* The Weizmann Institute of Science, http://www.weizmann.ac.il/)

Contributing Institution:
The Weizmann Institute of Science
http://www.weizmann.ac.il/

JPC Diagnoses:
1. Mesentery: Arteritis and periarteritis, necrotizing and eosinophilic, chronic, multifocal, severe, with arterial thrombi and rare larval spirurids.
2. Small intestine: Enteritis and peritonitis, necrotizing and eosinophilic, chronic, regionally extensive, severe.

JPC Comment:
The JPC's own MAJ Katie Scott moderated Conference 6 and took participants on a journey of cases from around the world; each one was from somewhere outside of the continental U.S., highlighting the truly global nature of the WSC and the importance of international contributions to pathology education. This first case provided an excellent opportunity to review of the pathogenesis and life cycle of *Spirocerca lupi*, both of which are well-covered in the contributor's comment. Additionally, the lesions of spirocercosis that are considered pathognomonic in the dog were covered and include aortic scarring with aneurysms, thoracic spondylitis, and caudal esophageal nodules. Special attention was paid to the chronic arterial thrombi present in numerous arteries in this case, which are a classic part of the pathogenesis of this parasite due to its arterial migratory routes and chronic intimal irritation. Participants were also reminded of the importance of specifying what type of vessels (arteries, arterioles, veins, lymphatics, etc.) are affected when giving a description, as this can provide important clues towards pathogenesis of some diseases that may preferentially affect a specific vessel type.

Spirocerca lupi is one of a handful of helminths that are classified as Group I carcinogens by the International Agency for Research on Cancer (IARC) due to the well-documented malignant transformation of S. *lupi* esophageal nodules into esophageal fibrosarcomas or osteosarcomas in up to 25% of infected dogs.[6] Less commonly, chondrosarcomas or undifferentiated pleomorphic sarcomas can also be seen.[6] Metastasis to multiple locations throughout the body, including the lungs, kidneys, stomach, spleen, heart, and tongue, occurs frequently.[6,7] Significantly higher levels of interleukin-8 (IL-8) have been documented in dogs with malignant esophageal nodules.[4] IL-8 is released by activated fibroblasts in pre-neoplastic nodules and is chemotactic for neutrophils. IL-8 is also involved in the tumor progression of human herpesvirus-4 (Epstein–Barr virus)-induced carcinomas.[4]

Other unwanted guests that no one invited to the party due to their classification as Group I carcinogens include *Clonorchis sinensis,*

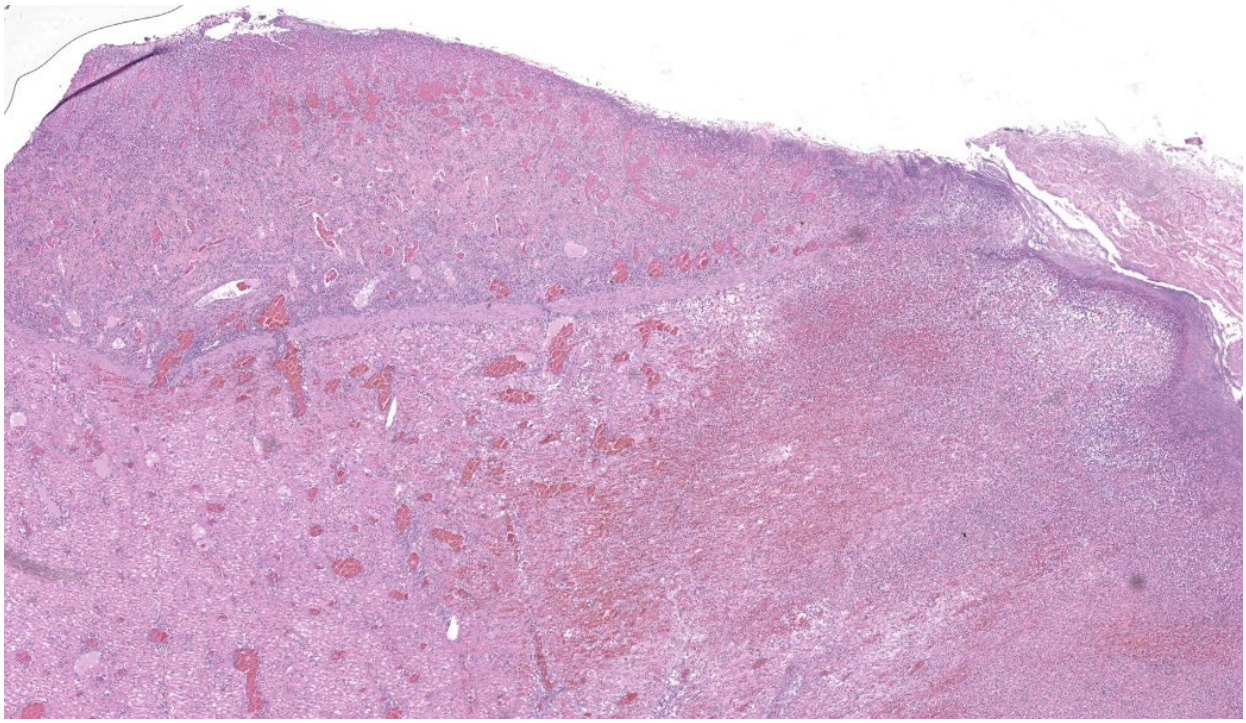

Figure 1-6: Jejunum, dog. There is full thickness necrosis of the mucosa and effacement of the normal architecture of the muscular tunics by granulation tissue in segments supplied by affected arterioles. (HE, 46X)

Opisthorchis viverrine, and *Schistosoma haematobium*. *Clonorchis sinensis*, a liver fluke transmitted via ingestion of undercooked fish hosting the parasitic metacercariae, can induce hepatocellular carcinomas or cholangiocarcinomas via mechanical damage to bile duct epithelial cells and suppression of biliary epithelial apoptosis via a wide range of excretory and secretory products (ESP).[6] *Opisthorchis viverrine,* another liver fluke ingested from raw fish, also induces cholangiocarcinoma through similar mechanisms to *C. sinensis*. *Schistosoma haematobium*, another trematode, causes squamous cell neoplasms within the urinary bladder and is the only human schistosome directly associated with cancer. *S. japonicum* and *S. mansoni* are also classified as carcinogens, but as Groups 2B and 3, respectively.[6]

Yet another parasite within veterinary species that is well-known to induce malignant neoplasms is *Cysticercus fasciolaris*, the larval form of the cestode *Taenia taeniaformis*. This larval tapeworm can induce the formation of fibrosarcomas in the liver of infected rats.[5] There is a short list of additional parasites associated with the development of neoplasia, but the body of literature has not yet established a direct causal link between these neoplasms and the parasites themselves. These include: *Trichosomoides crassicauda*, the urinary bladder threadworm of rats that, although not directly carcinogenic in and of itself, is associated with the development of urothelial carcinomas via the creation of a chronically irritated environment within the urinary bladder that may be more receptive to the effects of external carcinogens; *Heterakis gallinarum* and *H. isolonche*, cecal nematodes of avian

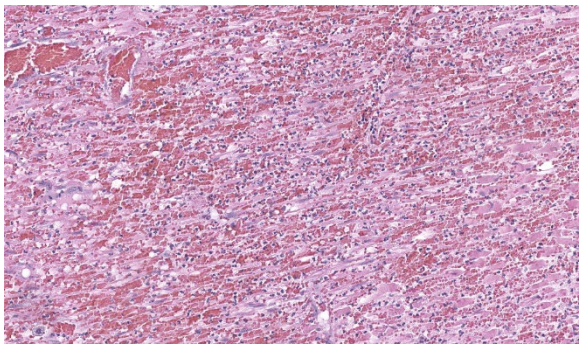

Figure 1-7: Jejunum. High magnification of the muscular tunic of the affected segment of intestine with degeneration, necrosis and atrophy of smooth muscle and proliferation of granulation tissue. (HE, 304X)

species, induce granulomatous nodule formation that can eventually progress to leiomyomas; and *Trichuris muris*, an intestinal-dwelling nematode of mice, can induce chronic cecal irritation that can develop into intestinal neoplasms.[5,8] Keeping these tiny not-friends on a short list of carcinogenic or cancer-associated parasites is crucial to the pathologist's differentials list when faced with cases where their consideration is warranted.

References:

1. Aroch I et al. Spirocercosis in dogs in Israel: A retrospective case-control study (2004-2009). *Vet Parasitol.* 2005;211:234-40.
2. Brown CC et al. Alimentary system. In: Jubb, Kennedy, and Palmer's Pathology of Domestic Animals, 5th edition; Maxie MG ed., Academic Press, Inc. Vol 2, 2007 pp. 97-98.
3. Du Plessis CJ et al. Aberrant extradural spinal migration of Spirocerca lupi: four dogs. J Small Anim Pract. 2007;48:275-8 (2007).
4. Long X, Ye Y, Zhang L, Liu P, Yu W, Wei F, Ren X, Yu J. IL-8, a novel messenger to cross-link inflammation and tumor EMT via autocrine and paracrine pathways (Review). Int J Oncol. 2016;48(1):5-12
5. Mahesh Kumar J, Reddy PL, Aparna V, Srinivas G, Nagarajan P, Venkatesan R, Sreekumar C, Sesikaran B. Strobilocercus fasciolaris infection with hepatic sarcoma and gastroenteropathy in a Wistar colony. Vet Parasitol. 2006;141(3-4):362-7.
6. Porras-Silesky C, Mejías-Alpízar MJ, Mora J, Baneth G, Rojas A. Spirocerca lupi Proteomics and Its Role in Cancer Development: An Overview of Spirocercosis-Induced Sarcomas and Revision of Helminth-Induced Carcinomas. Pathogens. 2021;10(2):124.
7. Sasani F et al. The evaluation of retrospective pathological lesions on spirocercosis (Spirocerca lupi) in dogs. J Parasit Dis. 2014;38:170–173.
8. Serakides R, Michel AF, de Lima Santos R, and Silva SM. Proliferative and inflammatory changes in the urinary bladder of female rats naturally infected with Trichosomoides crassicauda: Report of 48 cases. Arq Bras Med Vet Zootec. 2001;53(2).
9. Tudury EA et al. Spirocerca lupi-induced acute myelomalacia in the dog. A case report. Braz J Vet Res Anim Sci. 1995;32:22.

CASE II:

Signalment:
18 months old ewe, Merino, *Ovis aries*

History:
An experimental Merino CLN6 research flock was maintained at University of Sydney Farms, Camden, which was based on affected and carrier sheep that were sourced from two medium-wool Merino flocks in northern New South Wales.

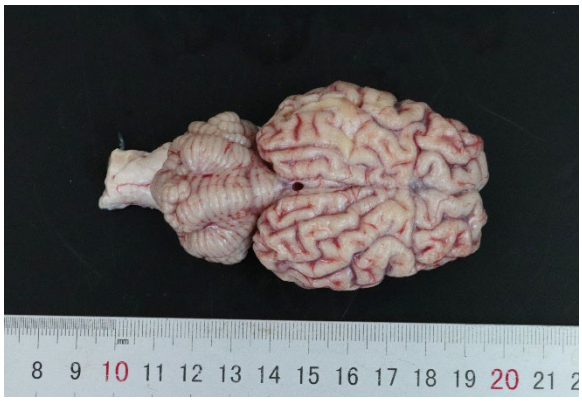

Figure 2-1: Brain, sheep. The cerebral hemispheres are small, firm and flattened dorsoventrally. The sulci are wider, and gyri were narrower than normal. There is diffuse, mild to moderate yellow discoloration (The University of Sydney, Veterinary Pathology Diagnostic Services http://sydney.edu.au/vetscience/vpds/)

This ewe developed clinical signs including decreased menace response, visual impairment, motor deficit and reduced herding instinct. The animal was euthanized.

Gross Pathology:
At postmortem examination the cerebral hemispheres were small, firm and flattened dorsoventrally. The sulci were wider, gyri were narrower than normal. There was diffuse, mild to moderate yellow discoloration.

Laboratory Results:
Missense mutation (c.184C > T; p.Arg62Cys) in ovine CLN6 gene detected by single nucleotide polymorphism (SNP) genotyping using a commercial SNP-Chip panel.

Microscopic Description:
Brain, frontal cortex: There is diffuse disruption of the laminar cortical architecture and diffuse atrophy of all layers, most apparent in the granular, pyramidal and ganglionic cell layers (mid-layers atrophy). The grey matter shows neuronal loss and diffuse moderate gliosis with increased numbers of astrocytes. The remaining neurons frequently contain variable numbers of up to 5 µm diameter, granular to globular, glassy, eosinophilic, intraneuronal bodies displacing large and often vesicular nuclei. Small neurons show hypereosinophilic cytoplasmic and pyknotic nuclei (necrosis).

Luxol fast blue (LFB): Intraneuronal storage material is LFB positive.

Periodic acid-Schiff (PAS): Intraneuronal storage material is PAS positive.

Contributor's Morphologic Diagnoses:
Brain, frontal cortex: Neuronal degeneration and loss, diffuse, moderate with intracytoplasmic ceroid accumulation and moderate astrocytosis, Merino, ovine.

Neuronal ceroid lipofuscinosis

Contributor's Comment:
Neuronal ceroid-lipofuscinoses are a heterogenous group of recessively inherited lysosomal storage diseases. In human medicine this neurodegenerative disease is referred to as Batten's disease and affects children.[1] This disease is characterized by atrophy of cerebral cortex, retina and cerebellar Purkinje system and accumulation of autofluorescent pigment in neurons and other cells. The pathogenesis

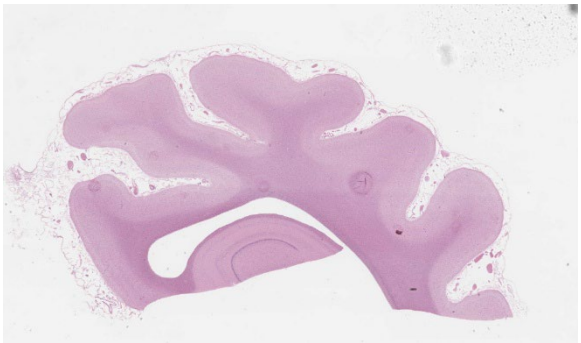

Figure 2-2: Diencephalon, sheep. There is diffuse separation and thinning of the cerebral gyri and dilation of the lateral ventricle (hydrocephalus ex vacuo) (HE, 10X)

of at least some forms of NCL may involve a defect in mitochondria rather than a defect in lysosomal catabolism and may involve accumulation of hydrophobic protein.[2]

Studies show that functional neuron loss is related to selective loss of specific neuron populations that is preceded by localized glial activation, and synaptic alterations. Rather than storage material accumulation, localized activation of glia is a better predictor of the distribution of subsequent neuron loss.[5,7] It is not clear whether this glial activation contributes to neuron loss or is a protective response, nevertheless it appears that neuroinflammation is a key part of the pathogenesis in many, if not all, forms of NCL.[10]

NCLs have been documented in a number of domestic animal species, including dogs, cats, cattle, and several breeds of sheep such as Merino, South Hampshire, Rambouillet and White Swedish Landrace.[3,6,9,11] Affected Merino sheep developed clinical signs between 7 months and a year of age. The ovine gene organization in this breed is very similar to that of human CLN6 (late infantile variant) and there is a high degree of homology between species along the whole coding length.[4] Active research studies utilize sheep flocks containing affected animals deliberately bred and maintained for studies relevant to human disease.

Contributing Institution:
The University of Sydney
University Veterinary Teaching Hospital Camden
https://www.univetscamden.com.au/
Veterinary Pathology Diagnostic Services
http://sydney.edu.au/vetscience/vpds/

JPC Diagnoses:
Cerebrum: Neuronal degeneration and loss, chronic, diffuse, severe, with cortical atrophy, neuronal intracytoplasmic pigment, mild astrocytosis, and hydrocephalus ex vacuo.

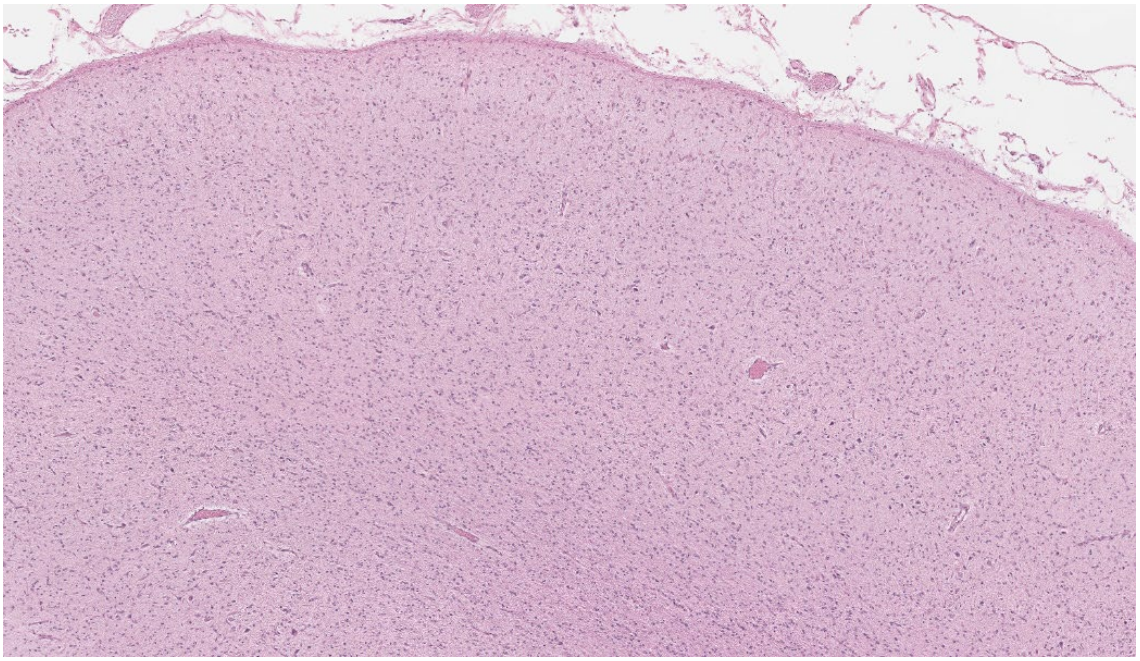

Figure 2-3: Diencephalon, sheep. There is a loss of normal stratification of neurons within the cortical gray matter. (HE, 65X)

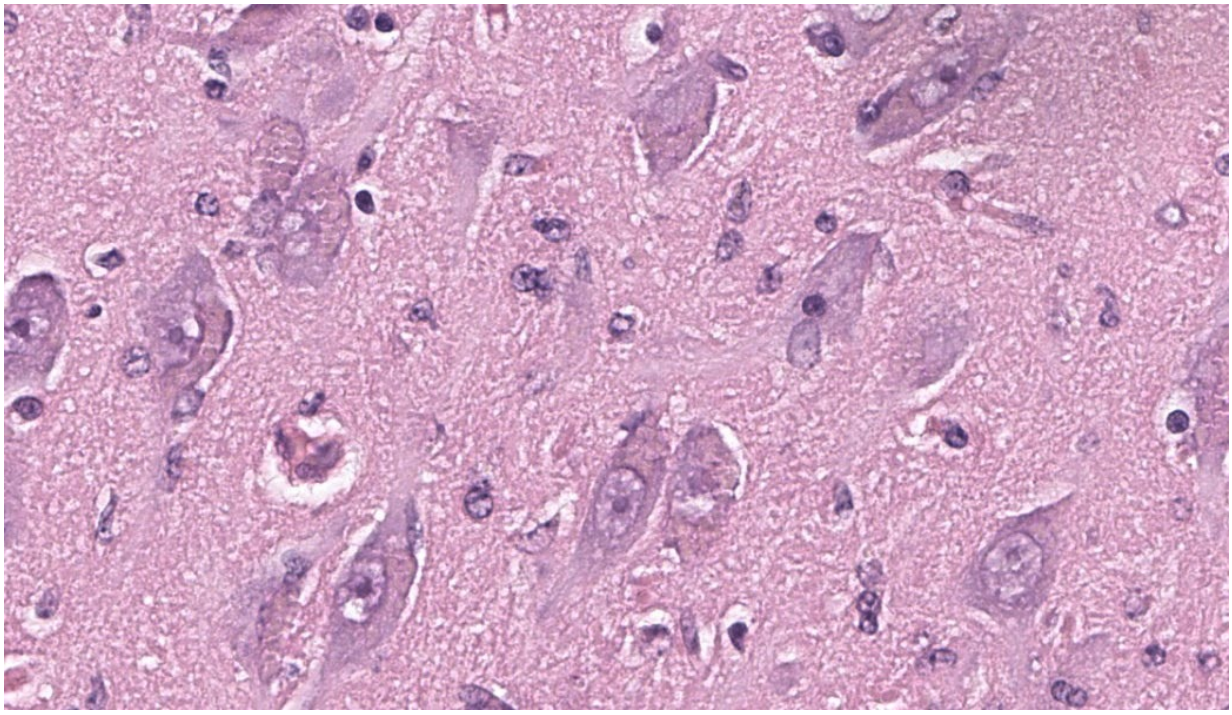

Figure 2-4: Diencephalon, sheep. Neuronal cytoplasm contains numerous amphophilic to brown 2um ceroid granules. (HE, 650X)

JPC Comment:

This classic case of ovine neuronal ceroid lipofuscinosis (NCL) stimulated great discussion on some of the histologic changes seen in the conference slide. It was the opinion of conference participants that there was true ventricular dilation evident histologically, likely secondary to the cerebral atrophy and parenchymal loss that is characteristic in this condition, leading to the development of a hydrocephalus *ex vacuo.* This brand of hydrocephalus is characterized by the ventricles filling with additional cerebrospinal fluid (CSF) in response to a vacuum created by the extra space from parenchymal loss. As the pathogenesis would imply, there is no accompanying increase in CSF pressure with this type of hydrocephalus as there is in other types.

One participant remarked that there was an increased number of visible axons within the affected grey matter. This posed the question of whether the increased visibility of axons was secondary to the neuronal loss from NCL or if there was true disorganization of the axons from the outset. The jury was split on this one, but the majority thought it was likely due to the former. A discussion on the intracytoplasmic storage material within neurons in this condition followed, including a review of the difference between lipofuscin and ceroid. Lipofuscin is considered a normal "wear and tear" pigment seen in long-lived cells and is not considered to be related to pathologic processes. Ceroid, however, is only seen in disease states and accumulates secondary to oxidative stress. The autofluorescent proteins in these cases are stored within lysosomes, which are unable to further break them down due to an endo-lysosome defect. In this case, in-house Luxol fast blue and PAS stains were performed, which nicely highlighted the intracytoplasmic accumulations.

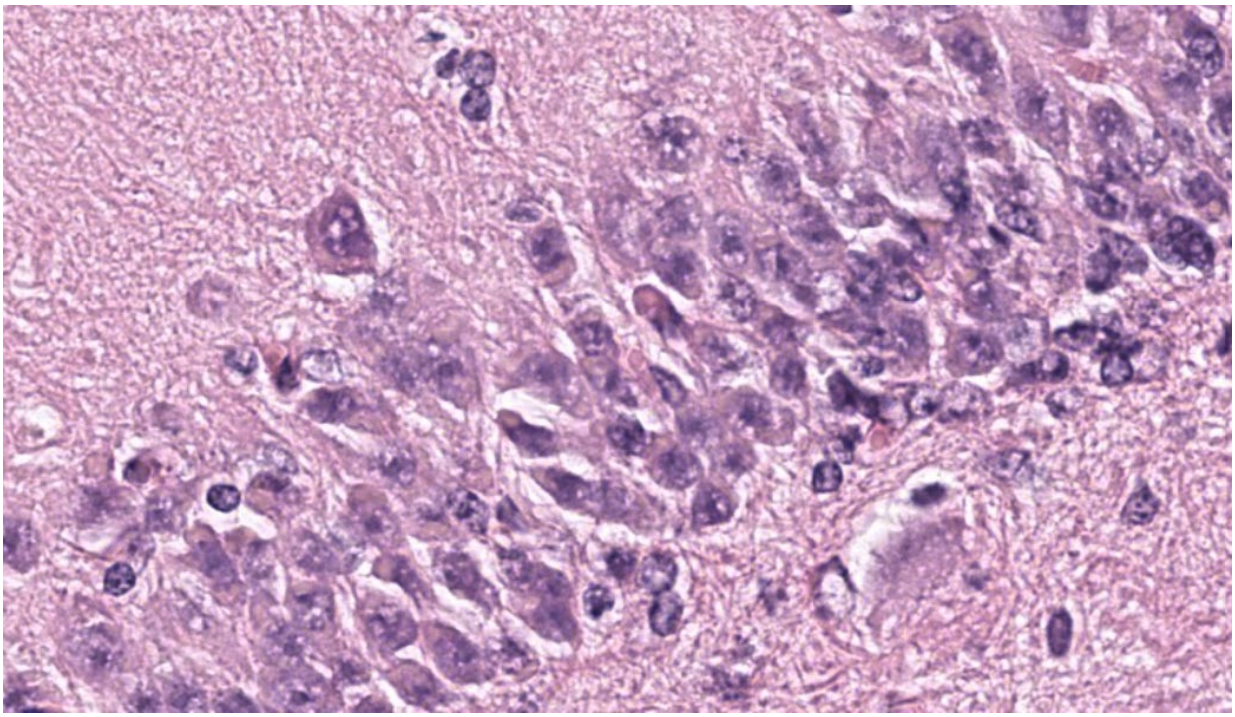

Figure 2-5: Diencephalon, sheep. Hippocampal neurons contains numerous amphophilic to brown 2um ceroid granules. (HE, 650X)

Currently, there are 13 different forms of NCLs documented in humans.[9] Each one has a distinct single-gene defect that affects the encoding of proteins in the endolysosomal system. These forms are generally classified into either soluble lysosomal enzyme/cytosolic protein deficiencies or insoluble transmembrane protein defects.[9] The lysosome is traditionally viewed as the 'waste-disposal' unit of the cell, but recent studies on NCLs has shown that the lysosomal system also plays critical roles in nutrient sensing and cellular homeostasis. This indicates that NCL mutations have wide effects on cellular functions in multiple organ systems, including autophagy and synaptic dysfunctions.[9] The use of animal models for NCLs has enabled researchers to identify the most susceptible neuronal populations and has demonstrated that glial cells are both negatively affected by and actively contribute to disease progression.[9]

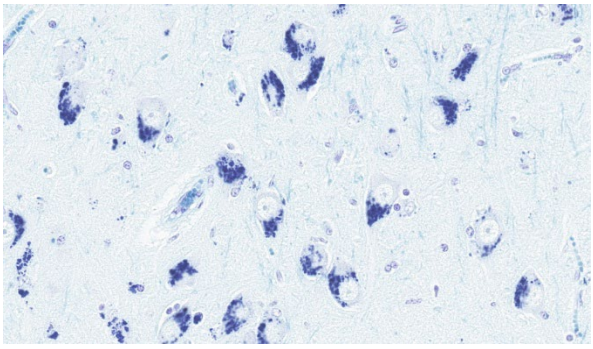

Figure 2-6: Diencephalon, sheep. A Luxol fast blue demonstrates the ceroid granules within neuronal cytoplasm. (Luxol fast blue, 650X).

References:

1. Anderson G, Elleder M, Goebel HH. Morphological diagnostic and pathological considerations. In: In: Mole SE, Williams RE, Goebel HH, ed. The Neuronal Ceroid Lipofuscinoses (Batten Disease). 2nd ed. New York, NY: Oxford University Press; 2011:35-36.
2. Cantile C, Youssef, S. Nervous system. In: Maxie MG, ed. Jubb, Kennedy, and

Palmer's Pathology of Domestic Animals. Vol 1. 6th ed. St. Louis, MO: Saunders Elsevier; 2016:290-291

3. Chalkley MD, et al. Characterization of neuronal ceroid-lipofuscinosis in 3 cats. *Vet Pathol*. 2014;51(4):796-804.
4. Chalkley MD, et al. Characterization of neuronal ceroid-lipofuscinosis in 3 cats. *Vet Pathol*. 2014;51(4):796-804.
5. Cook RW, Jolly RD, Palmer DN, Tammen I, Broom MF, McKinnon R. Neuronal ceroid lipofuscinosis in Merino sheep. *Aust Vet J*. 2002;80:292–297.
6. Cooper JD, Russell C, Mitchison HM. Progress towards understanding disease mechanisms in small vertebrate models of neuronal ceroid lipofuscinosis. *Biochim Biophys Acta.* 2006;1762(10):873-889.
7. Jolly RD, Martinus RD, Palmer DN. Sheep and other animals with ceroid-lipofuscinoses: their relevance to Batten disease. *Am J Med Genet*. 1992;42(4):609–614.
8. Kay GW, Palmer DN, Rezaie P, Cooper JD. Activation of non-neuronal cells within the prenatal developing brain of sheep with neuronal ceroid lipofuscinosis. *Brain Pathol*. 2006;16(2):110-116.
9. Nelvagal HR, Lange J, Takahashi K, Tarczyluk-Wells MA, Cooper JD. Pathomechanisms in the neuronal ceroid lipofuscinoses. *Biochim Biophys Acta Mol Basis Dis*. 2020;1866(9):165570.
10. O'Brien DP, Katz ML. Neuronal ceroid lipofuscinosis in 3 Australian Shepherd littermates. *J Vet Intern Med.* 2008;22(2):472–475.
11. Palmer DN, Barry LA, Tyynelä J, Cooper JD. NCL disease mechanisms. *Biochim Biophys Acta.* 2013;1832(11):1882-93.
12. Palmer DN, Tammen I, Drogemuller C, et al. Large animal models. In: Mole SE, Williams RE, Goebel HH, ed. The Neuronal Ceroid Lipofuscinoses (Batten Disease). 2nd ed. New York, NY: Oxford University Press;2011:284–320.

CASE III:

Signalment:
9 year 7 months old, male neutered, domestic short haired cat, Felis Cattus.

History:
Presented in March for progressive lethargy, anaemia and thrombocytopenia. CT scan showed lung and splenic abnormalities. A splenectomy was performed and histology

Figure 3-1: Lung, cat. Diffusely, all lung lobes are markedly expanded by moderately firm red-cream tissue. The pleural surfaces are smooth despite the lungs being expanded. (Photo courtesy of: Department of Veterinary Medicine, University of Cambridge, www. vet.cam.ac.uk)

(external laboratory) was suggestive of histiocytic disease. Lomustine treatment was started, and the animal was euthanised in May after progressing to respiratory distress.

Gross Pathology:
Diffusely all lung lobes were markedly expanded by moderately firm red-cream tissue. The pleural surfaces were smooth despite the lungs being expanded.

The pericardial sac contained approximately 2mL of serosanguinous fluid. The heart weighed 28 g (cardiomegaly, <20g is considered normal). Cross section of the left ventricular free wall, interventricular septum, and right ventricular free wall measured 6 mm, 6 mm, 3 mm respectively (cardiac hypertrophy with right ventricular free wall most prominently affected). This results in a ratio between the chamber widths of 2:2:1. The left and right auricles were approximately 15 mm in length and width, and 5-10 mm in depth, and were both similar sizes (bilateral auricular dilation).

Laboratory Results:
Anaemia and thrombocytopenia diagnosed on haematology at first presentation in March to the referring vet practice.

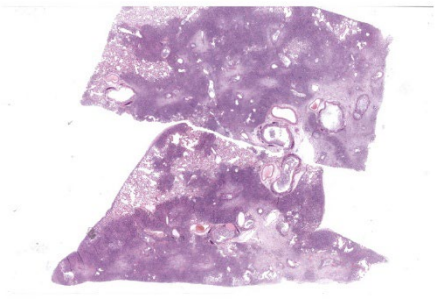

Figure 3-2: Lung, cat. Two sections of consolidated lung are submitted for examination. There is an extensive alveolar infiltrate which affects approximately 90% of the section. (HE 10X).

Microscopic Description:
Expanding the airway and alveolar interstitium, subpleural spaces and also filling alveolar spaces, there is a proliferation of large numbers of round-polygonal cells. The proliferative round cell population have a moderate amount of eosinophilic cytoplasm and a reniform nucleus that contains coarsely stippled chromatin and a single nucleolus. There is mild anisocytosis and anisokaryosis, and there are occasional multinucleated cells. There is one mitotic figure per 2.37 square mm. Within the pleural, peribronchiolar interstitium and alveolar septa, the proliferative cells are accompanied by fine strands of collagen, resulting in further expansion of those structures, and in some areas, complete effacement of the normal pulmonary architecture with obliteration of air spaces. In non-consolidated areas, alveolar septa are multifocally ruptured (microscopic emphysema). There is multifocal, moderate, hyperplasia of bronchiolar smooth muscle, and occasionally, especially in subpleural areas, there is type 2 pneumocyte hyperplasia. Medium-sized pulmonary arteries demonstrate hyperplasia of the tunica media. Airway epithelium is frequently sloughed (post-mortem artefact). Gram, Ziehl-Neelson and PAS-stained sections do not highlight micro-organisms.

Contributor's Morphologic Diagnoses:
Lung, feline pulmonary histiocytosis

Etiological diagnosis: Feline pulmonary Langerhans cells histiocytosis

Contributor's Comment:
Feline pulmonary Langerhans cell histiocytosis is a proliferative disorder of Langerhans cells predominantly affecting the lung. The process is progressive, with animals ultimately developing fatal respiratory compromise. The condition has been reported to have

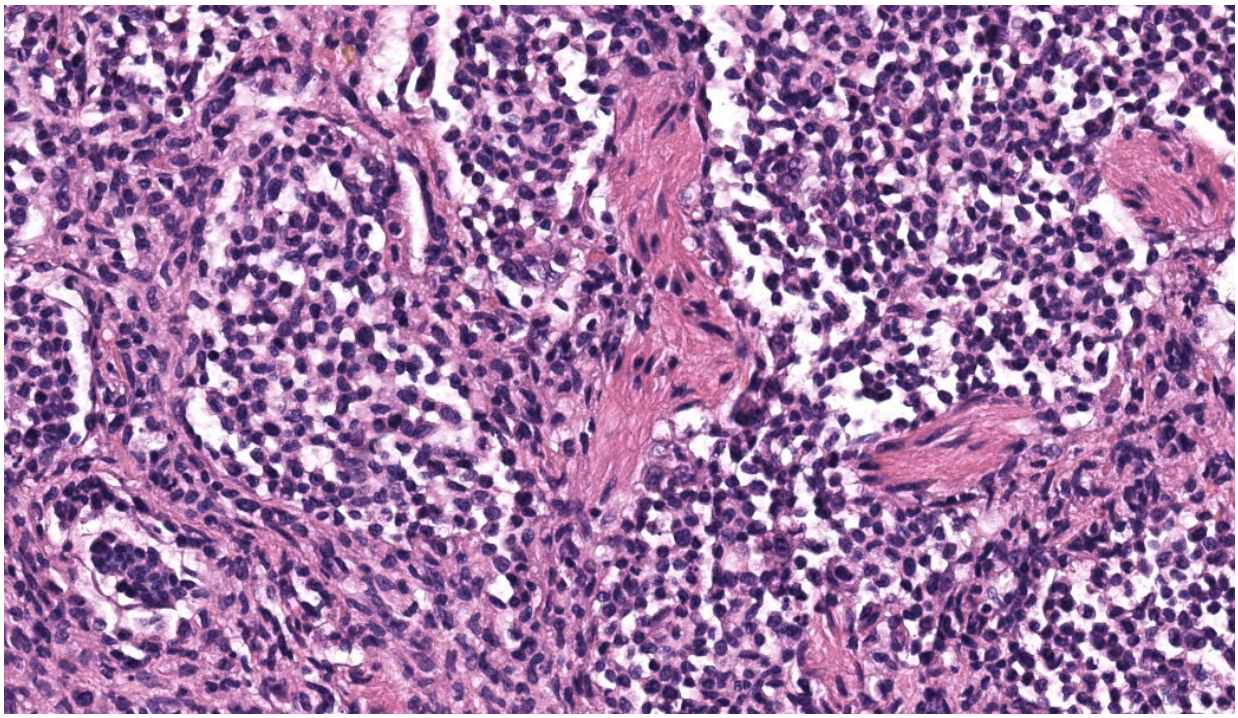

Figure 3-3: Lung, cat. In affected areas, alveoli are filled by sheets of histiocytes. Intervening septa are expanded by congestion, edema, fibrous connective tissue, and there is smooth muscle hyperplasia. (HE 597X).

multi-organ involvement and may affect the spleen, as in this case.[3]

Initial clinical signs of feline pulmonary Langerhans cell histiocytosis are variable but ultimately progress to a restrictive dyspnoea.[1] The insidious onset and unspecific clinical signs means that definitive diagnosis in live patients is challenging. Langerhans cells express CD1a, MHC-class 2, langerin (CD207) and E-cadherin.[6,8]

In humans, the condition is associated with young adults who smoke. The exact pathogenesis of the condition is uncertain.[3] Current evidence from human medicine suggests the underlying process is a myeloid neoplasm with inflammatory properties, which may regress or progress in response to cessation of smoking.[13] In cats, reactivity or neoplastic has not been defined.

The condition generally affects middle aged to older cats, with an interstitial and alveolar pattern on lung imaging.[1] Similar to the eccentric cardiac hypertrophy in this case, occasionally cats with Feline progressive pulmonary histiocytosis develop right ventricular hypertrophy and right auricle dilation due to the increase in pulmonary pressure.[14]

Grossly, lungs have an expanded non-collapsing texture and contain multifocal pale red-cream coalescing masses, which can be very extensive in distribution. In advanced cases the entire lung lobes can be affected, with extension of masses into the pleura.[12] The pancreas, kidney, liver and local or remote lymph nodes may also contain similar mass lesions.[2]

Typical microscopic findings include pleomorphic histiocytic cells that target terminal and respiratory bronchioles and extend into

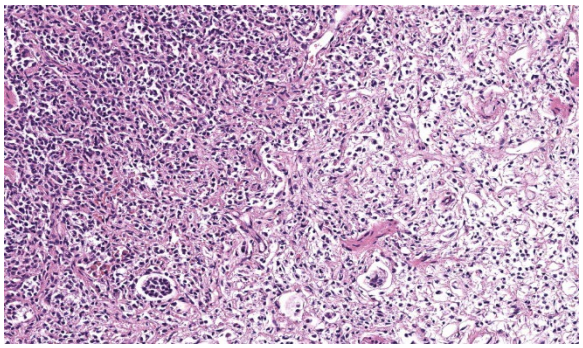

Figure 3-4: Lung, cat. In less affected areas (at right), there are fewer histiocytes, and alveolar parenchyma is effaced by edema and fibrosis. (HE, 333X).

adjacent alveoli.[3] Affected bronchioles undergo smooth muscle hyperplasia and there is fibrosis of the alveolar septa. The Langerhans cells demonstrate CD18 and E-cadherin, vimentin and IBA-1positive immunoreactivity.[1] In addition, feline Langerhans cells do not react to CD204.[7]

The presence of Birbeck granules in the cytoplasm ultrastructurally is characteristic of the Langhans cell phenotype in cats.[3,4] Birbeck granules are the langerin (CD207) receptor cross-linked to antibody and subsequently internalised from the cell surface membrane.[9] Canine Langerhans cells do not contain Birbeck granules.[12]

Feline pulmonary Langerhans cell histiocytosis has been diagnosed on the basis of BAL cytology and pulmonary radiographs.[9] Thoracic radiographs have miliary to nodular radiodense foci in a bronchointerstitial pattern.[10]

Other progressive histiocytic diseases that affect the lungs include progressive histiocytosis in cats, and cutaneous Langerhans histiocytosis or systemic histiocytosis in dogs.[10] The microscopic appearance between canine and feline Langerhans histiocytosis in the lungs is similar, with a primary focus on terminal bronchioles.[12] Feline progressive pulmonary histiocytosis has been reported in a lion,[14] and focal Langerhans cell histiocytosis, without lung involvement, has been reported in the pancreas of a cat.[11]

Contributing Institution:
University of Cambridge, Madingley Road, Cambridge UK

JPC Diagnoses:
Lung: Histiocytosis, alveolar, chronic, diffuse, severe, with fibrosis and smooth muscle hyperplasia.

JPC Comment:
The contributor does an excellent job of summarizing this condition in cats and cross-comparing with a few other species affected by a similar process (including humans). Many of the topics mentioned in their write-up were focal points of discussion during conference, including key histologic features, IHC immunoreactivity profile, and ultrastructural findings.

Langerhans cells are antigen-presenting dendritic cells (DC) derived from CD34+ precursors in the bone marrow. They eventually make their way to and reside in the epidermis and epithelium of the oral cavity, vagina, and bronchial mucosa of the lung.[3] Upon contacting and internalizing an antigen, Langerhans cells will migrate to regional lymph nodes and present their cool find (the antigen) to naïve CD4+ T-cells using major histocompatibility complex (MHC) class II. The characteristic "Birbeck's granules" seen on electron microscopy (EM) are five-layered, rod-shaped cytoplasmic organelles that kind of resemble hot dogs on a bun and are present only within Langerhans cells. These granules are formed by the internalization of CD207, normally found on the surface of Langerhans cell.

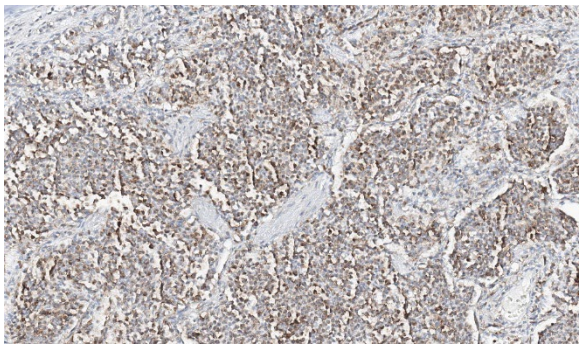

Figure 3-5: Lung, cat. Histiocytes within alveoli demonstrate strong cytoplasmic immunoreactivity for IBA-1) (anti-IBA1, 328X).

CD207 is a C-type lectin also known as "langerin" that assists with recognition of pathogen-associated molecular patterns (PAMPs), internalization of an antigen, and further stimulating an immune response as described above.[3]

While the pathogenesis of feline pulmonary Langerhans cell histiocytosis is not yet fully understood, in humans, one of the main hypotheses for pulmonary Langerhans cell histiocytosis is that of the "cytokine storm".[3,5] This hypothesis suggests that T-lymphocytes and Langerhans cells within the lungs produce a mutually amplifying cytokine cascade that drives recruitment, maturation, and proliferation of Langerhans cells in this condition.[5] Whether or not this fits within a reactive or neoplastic process remains to be seen, and some studies suggest assessing the clonality of the Langerhans cells in future research to try and make that distinction.[3]

References:

1. Argenta FF, de Britto FC, Pereira PR, et al. Pulmonary Langerhans cell histiocytosis in cats and a literature review of feline histiocytic diseases. *J Feline Med Surg*. 2020;22(4):305-312.
2. Bellamy E, Di Palma S, Ressel L, et al. Disseminated Langerhans cell histiocytosis presenting as oesophageal disease in a cat. JFMS Open Rep. 2019;5(2):2055116919874902.
3. Busch MD, Reilly CM, Luff JA, et al. Feline pulmonary Langerhans cell histiocytosis with multiorgan involvement. Vet Pathol. 2008;45(6):816-24.
4. Caswell JL, Williams KJ. Respiratory System. In: Maxie MG, ed. Jubb, Kennedy, and Palmer's Pathology of Domestic Animals. Vol 2. 6th ed. Philadelphia, PA: Elsevier Ltd. 2016:499.
5. Egeler RM, Favara BE, van Meurs M, Laman JD, Claassen E. Differential In situ cytokine profiles of Langerhans-like cells and T cells in Langerhans cell histiocytosis: abundant expression of cytokines relevant to disease and treatment. Blood. 1999;94(12):4195-201.
6. Fulmer AK, Mauldin GE. Canine histiocytic neoplasia: an overview. Can Vet J. 2007;48(10):1041-3,1046-50.
7. Hirabayashi M, Chambers JK, Sumi A, et al. Immunophenotyping of nonneoplastic and neoplastic histiocytes in cats and characterization of a novel cell line derived from feline progressive histiocytosis. Vet Pathol. 2020;57(6):758-773.
8. Laman JD, Leenen PJ, Annels NE, et al. Langerhans-cell histiocytosis 'insight into DC biology'. Trends Immunol. 2003;24(4):190-6.

9. Mau A, Chiu ES, Armien A, et al. Antemortem cytologic diagnosis of pulmonary Langerhans cell histiocytosis in a cat. Vet Clin Pathol. 2023;52(4):691-697.

10. Moore PF. A review of histiocytic diseases of dogs and cats. Vet Pathol. 2014;51(1):167-84.

11. Rissi DR, Brown CA, Gendron K, et al. Pancreatic Langerhans cell histiocytosis in a cat. J Vet Diagn Invest. 2019;31(6):859-863.

12. Valli VEO, Kiupel M, Bienzle D. Hematopoietic System. In: Maxie MG, ed. Jubb, Kennedy, and Palmer's Pathology of Domestic Animals. Vol 3. 6th ed. Philadelphia, PA: Elsevier Ltd. 2016 245-247.

13. Vassallo R, Harari S, Tazi A Current understanding and management of pulmonary Langerhans cell histiocytosis Thorax 2017;72:937-945.

14. Zhang L, Chen H, Ding Y, et al. Pulmonary Langerhans Cell Histiocytosis in an African Lion: A Rare Case Report. Animals (Basel). 2024;14(7):1011.

CASE IV:

Signalment:
Dromedary camel (*Camelus dromedarius*), adult female

History:
A lactating adult dromedary camel was one of two breeding females which had been recumbent for the last 2 to 4 days; both were in poor body condition. Other camels in the breeding herd were also in low body condition. Both recumbent animals were eating, drinking and were up to date with vaccinations. There had been no change in condition in response to worming and anticoccidial treatments. A pasture assessment was conducted, and the amount of feed available was determined to be inadequate for the lactating camels. Bloods were taken from both camels and supplementary feeding initiated.

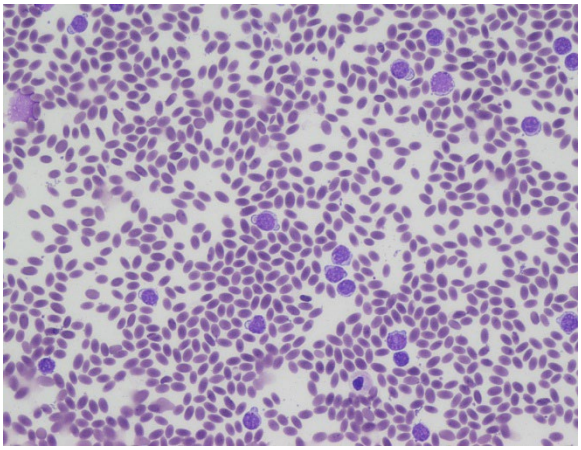

Figure 4-1: Blood smear, camel. Numerous atypical lymphocytes were present in the blood smear (Diff Quik, 400X). (Photo courtesy of: New South Wales Department of Primary Industries, Menangle,NSW2568 https://www.dpi.nsw.gov.au/about-us/science-and-research)

The second camel began to put on weight and became ambulatory after supplementary feeding, however the first female camel was unable to rise without assistance and continued to loose condition. The animal was euthanized and a post mortem conducted.

Gross Pathology:
Necropsy examination revealed that the ventral 40-50% of both lungs were pale-pink to white with a firm consistency and smooth surface on cross section. The paratracheal and parabronchial lymph nodes were diffusely markedly enlarged and were white on the cut surface. Other viscera appeared grossly normal.

Laboratory Results:

Hematology

On the blood smear collected during the initial clinical exam, numerous large atypical lymphocytes were observed throughout the smear.

Test	Normals	Units	Female camel 1 (euthanized)	Female camel 2 (recovered)
PCV (%)	27-45	%	24	22
RBC	10.5-17.2	10^{12}/L	6.32	5.76
Hemoglobin	11.3-19.0	g/dL	11.0	9.2
MCV	22-29.5	fL	38	38
MCHC	38-46	g/dL	46	42
MCH	9.6-12	pg	17	16
WBC	6.0-20.9	10^9/L	194.6	19.3
Neutrophils	2.0-13.3	10^9/L	21.41	17.18
Band Neutrophils	0.0-2.9	10^9/L	0	0
Lymphocytes	2.1-6.8	10^9/L	173.19	2.12
Monocytes	0.0-0.6	10^9/L	0.0	0.0
Eosinophils	0.0-3.0	10^9/L	0.0	0.0
Basophils	0.0-0.3	10^9/L	0.0	0.0
Nucleated RBC		/100wbc	0	Occasional
Reticulocytes		%	0	1
Platelets			Adequate	Adequate

Serum Biochemistry

Test	Normals	Units	Female camel 1 (euthanized)	Female camel 2 (recovered)
GGT	0-60	U/L	19	17
GLDH	0-20	U/L	4	4
AST	0-320	U/L	123	150
Bilirubin	0.1-3.2	µmol/L	2.0	3.1
CK	0-750	U/L	423	1693
Urea	5.0-12.4	mmol/L	11.1	9.4
Creatinine	0-288	µmol/L	101	119
Phos	1.5-3.4	mmol/L	1.2	1.98
Urea/Creatinine	0.00-0.07		0.11	0.08
Protein	54.0-75.0	g/L	53.8	48.1

Test	Normals	Units	Female camel 1 (euthanized)	Female camel 2 (recovered)
Albumin	25.0-45.0	g/L	16.2	20.4
Globulins	15.9-41.0	g/L	37.6	27.7
Albumin/Globulins	1.3-3.3		0.4	0.7
β-Hydroxybutyrate	0.00-0.50	mmol/L	0.02	0.01
Calcium	1.9-2.7	mmol/L	2.1	2.11
Magnesium	0.7-1.3	mmol/L	0.96	0.92
Haptoglobin	1.0-2.0	g/L	0.69	0.58
Serum Hemoglobin	0.0-0.2	g/dL	0.04	0.04
Glutathione Peroxidase	15-200	U/gHb	69	170

Bacterial Culture, Lungs
Moderate pure growth of *Streptococcus agalactiae*
Enzootic Bovine Leukosis ELISA
Camel 1 seronegative

Immunohistochemical markers

Marker	Cell type	Tissue	Number of positive cells	Positive cell distribution
CD79b	B Cell	Lung	+++	Majority of cells within neoplastic infiltrate, scattered cells within peribronchial and peribronchiolar spaces, interlobular and alveolar septae and alveolar lumen
		Lymph node	+++	The majority of cells within the cortex and moderate numbers (30-50% of cells) within the medulla
		Spleen	+++	Majority of cells within red and white pulp
CD3	T Cell	Lung	+	Scattered throughout parenchyma, and small numbers accompanying neoplastic infiltrate
		Lymph node	++	Moderate numbers multifocally throughout the medulla
		Spleen	+	Predominantly around blood vessels

Microscopic Description:
Camel; Lung
Description Multifocally throughout the section, expanding the lamina propria of larger airways, multifocally invading the airway epithelium, expanding numerous alveolar septae and infiltrating into interlobular septae and the pleural space, there is a densely cellular lymphoid neoplasm. The neoplasm is made up of sheets and rows of closely packed round cells supported by a fine pre-existing fibrous stroma. The neoplastic cells contain nuclei 5-7µm in diameter and have indistinct cytoplasmic borders, scant amphophilic cytoplasm, round to ovoid paracentral nuclei with coarsely clumped chromatin with moderate numbers of cells possessing a single nucleolus. Throughout the neoplastic cells there is mild anisokaryosis and anisocytosis. Mitotic figures numbering 5 per 2.37mm^2 with occasional bizarre mitoses. Multifocally the neoplastic cells closely surround and infiltrate the tunica media of small blood vessels. Numerous alveolar spaces are filled with eosinophilic

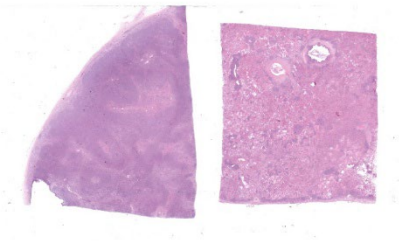

Figure 4-2: Lymph node, lung, camel. At subgross magnification, there is an cellular infiltrate in both organs which effaces normal architecture. (HE, 5X)

fibrillar material (fibrin) admixed with abundant neutrophils and foamy macrophages, while others contain large amounts of homogenous eosinophilic material (edema). Multifocally some alveolar spaces are expanded and ruptured (emphysema). Bronchioles contain moderate numbers of neutrophils and macrophages admixed with strands of hypereosinophilic fibrillar material (fibrin) with neutrophils transmigrating across the respiratory epithelium. There is occasional loss of type I pneumocytes with replacement by type II pneumocytes.

Camel; Paratracheal Lymph Node
Description Multifocally the normal architecture of the cortex, paracortex and medulla is disrupted and replaced by a densely cellular neoplasm composed of lymphoid cells. The neoplasm is comprised of sheets of closely packed small round cells with nuclei 5-7µm in diameter. Cells are mostly round with indistinct cytoplasmic margins, scant basophilic or eosinophilic cytoplasm, high nuclear to cytoplasmic ratio, and a paracentric nucleus with coarsely clumped chromatin. There is mild anisocytosis and anisokaryosis. There is an average of 12 mitoses per 2.37mm^2. Within the capsule of the lymph node there are small aggregates of neoplastic cells organized into sheets.

Contributor's Morphologic Diagnoses:
Lung and Lymph node; B-cell lymphoma
Lung; bronchopneumonia, fibrinosuppurative, multifocal, severe, subacute, with type II pneumocyte hyperplasia.

Contributor's Comment:
In this case, neoplastic cells were also found in the liver, spleen and heart of the camel. No neoplastic cells were found in the kidneys or in two sections of bone marrow (rib and sternum). The presence of atypical lymphocytes within the peripheral blood collected at the initial clinical examination greatly aided the diagnosis of lymphoma or leukemia in this case (Figure 1) and allowed the clinician to understand why this animal did not improve like the others in the herd once nutrition was improved. The neoplastic cells observed in the peripheral blood was suspected to be secondary to the lymphoma, given that no neoplastic cells were found within the bone marrow of the bones examined histopathologically. Leukemia is a feature of less than 20% of lymphomas in animals and is more commonly a feature of T-cell lymphomas.[9] Leukemia is most likely observed when the lymphoma invades the bone marrow or spleen, the latter of which contained neoplastic cells in this case.[9] In this

Figure 4-3: Lymph node, camel. The nodal architecture to include the cortex, paracortex, and medullary sinuses are expanded and/ effaced by a round cell neoplasm. (HE, 10X)

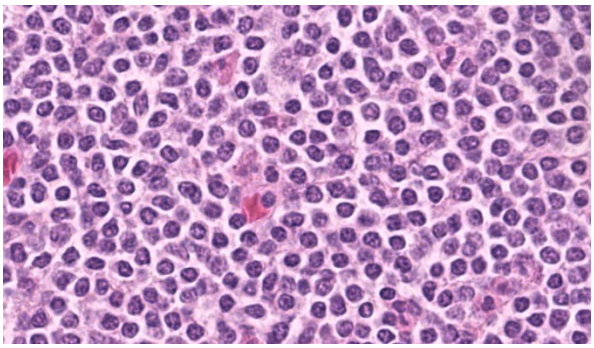

Figure 4-4: Lymph node, camel. High magnification of neoplastic lymphocytes. (HE, 1800X)

case a B-cell phenotype was confirmed via immunohistochemistry (Figures 7-11).

There are only a few reports in the literature describing lymphoma in dromedary camels. Similar to this case, the disease is typically reported in adult animals (>7 years) and has been reported in both male and female camels. Common clinical presentations include weight loss, anorexia, polyuria and polydipsia, with one report also describing peripheral lymphadenopathy and bilateral masses in the conjunctiva of one animal.[3,4,6] Peripheral lymphocytosis, sometimes with significant atypia in circulating lymphocytes and lymphoblasts, has been reported occasionally but is not always a feature of the disease in dromedary camls.[3,7]

Necropsy findings typically include disseminated nodules which can be found in various organs including the liver, spleen, lungs, kidneys, bladder and intestines. Often multiple mesenteric and/or mediastinal lymph nodes are enlarged.[3,4,6]

Histologically, lymphomas in dromedary camels are described as a highly cellular neoplasm often effacing the normal architecture of the tissues, made up of sheets of lymphoid cells with scant cytoplasm and distinct cell margins. There is some variability in the cellular morphology including anisocytosis and anisokaryosis, indistinct nucleoli to multiple nucleoli present and in one case multinucleated cells were observed.[3,4,6]

In contrast to this case, all cases in the literature from dromedary camels were identified as T-cell lymphomas. In those cases, lymphocyte lineage identification was performed using immunohistochemistry and identified the neoplastic cells as CD3 (pan T-cell) positive and either CD20 or CD79a (pan B-cell markers) negative.[3,4] More recently, flow cytometry has been used to further classify a multicentric T-cell lymphoma as a gd T-cell lymphoma and a combination of CD4 and WC-1 markers.[4] Other markers which have been used in the literature to differentiate round cell neoplasms in camelids include PAX-5, CD79b (B-cell markers), CD5 (T-cell marker), MUM1 (plasma cell marker), CD18 and CD68 (histiocyte markers).[1,4,6,8]

In other camelids (llamas and alpacas), lymphoma is identified as one of the most common types of neoplasia, and both T-cell and B-cell as well as non-T and non-B cell lympho

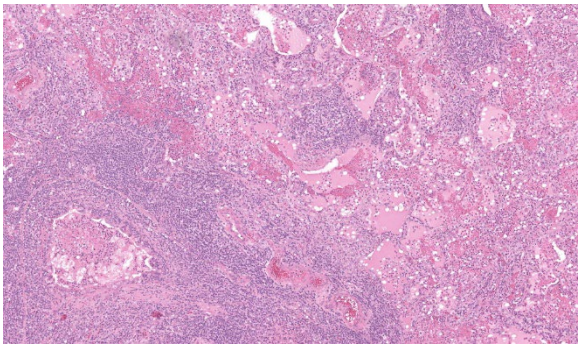

Figure 4-5: Lung, camel. Neoplastic lymphocytes infiltrate the walls of airways, efface BALT, surround vessels, and markedly expand alveolar septa (HE, 152X)

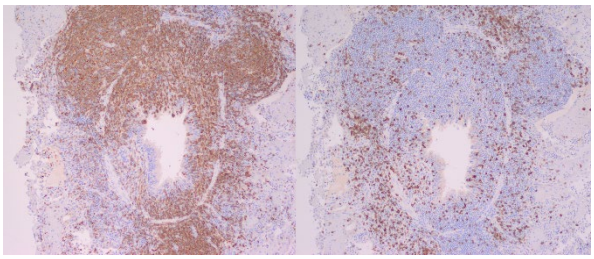

Figure 4-6: Lung, camel. Left: CD79b-positive lymphocytes surrounding and infiltrating into the epithelium of an airway (anti-CD79b, 100x). Right: Only relatively low numbers of CD3 positive lymphocytes are scattered throughout the lung (anti-CD3, 100x). (Photo courtesy of: New South Wales Department of Primary Industries, Menangle, NSW, 2568 https://www.dpi.nsw.gov.au/about-us/science-and-research/centres/emai)

mas have been reported.[1,8] Disseminated lymphoma has been reported in juvenile alpacas[1]

and lymphoma of the liver has been reported in a juvenile llama.[8] Multicentric lymphoma has been reported in both adult alpacas and llamas and the distribution of lesions in organs is similar to that described for dromedary camels with lesions also seen in the spleen, stomach, trachea and bone marrow.[1,8]

Contributing Institution:
Elizabeth Macarthur Agricultural Institute
New South Wales Department of Primary Industries,
Woodbridge Road, Menangle, NSW, 2568

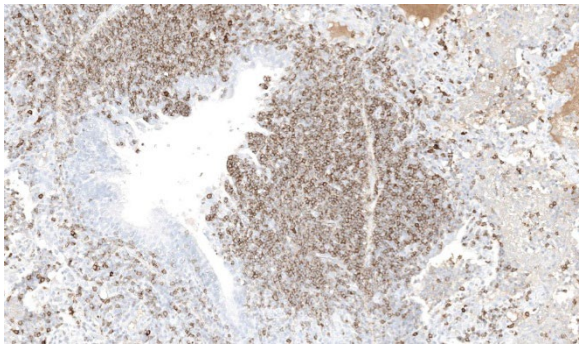

Figure 4-7: Lung, camel. Neoplastic cells infiltrating an airway demonstrate strong membranous immunoreactivity for CD20, a B-cell marker. (anti-CD20, 263X)

https://www.dpi.nsw.gov.au/dpi/about-us/research-and-development

JPC Diagnoses:
1. Lymph node and lung: Lymphoma.
2. Lung:Bronchopneumonia, fibrinosuppurative, subacute, multifocal, severe, with type II pneumocyte hyperplasia.

JPC Comment:
This camel just had to be contrarian in that it had a lymphoma of B-cell origin instead of T-cell like almost every other camel lymphoma out there. This case provided a great two-fer of a late-stage lymphoma and bronchopneumonia, and the contributor provides a thorough and well-written comment on lymphomas in camels.

Another primary point of discussion, and one that was briefly mentioned by the contributor, was the classification of this case as a lymphoma a leukemia given that there were intravascular atypical lymphocytes. Given that there was no bone marrow involvement, though, a lymphoma was the consensus. According to the WHO guidelines in dogs, a stage 5 lymphoma is characterized as generalized lymphadenopathy (involving both thoracic and abdominal nodes) with hepatosplenomegaly and involvement of either bone marrow, the CNS, or another extranodal site (such as the lungs).[10] This stage would best fit with the histologic findings in this case, as there was multiorgan involvement. Stage V is further classified into 5a or 5b, with either no clinical signs or apparent clinical illness, respectively, which would classify this camel's lymphoma as a stage 5b due to the obvious clinical signs described in her case. In human medicine, the fifth stage is not utilized; their

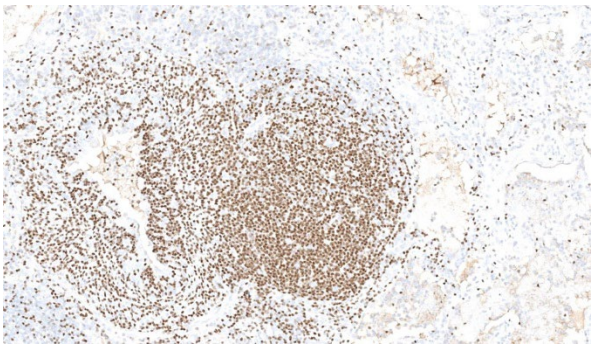

Figure 4-8: Lung, camel. Neoplastic cells infiltrating an airway demonstrate strong nuclear immunoreactivity for PAX5, a B-cell marker. (anti-PAX5, 263X)

grading scheme ends at stage 4.[5] Whether either (or neither) of these classification schemes fits with lymphoma in camelids, however, is currently unknown and will require additional studies.

References:

15. Aboellail TA. Pathologic and immunophenotypic characterization of 26 camelid malignant round cell tumors. J Vet Diagn Invest. 2013;25(1):168–172.

16. Desmirean M, Deak D, Rus I, Dima D, Iluta S, Preda A, Moldovan T, Roman A, Tomuleasa C, Petrushev B. Paraneoplastic hypereosinophilia in a patient with peripheral T cell lymphoma, not otherwise specified. Med Pharm Rep. 2019;92(4):421-426.

17. Heather A. Simmons, Scott D. Fitzgerald, Matti Kiupel, David R. Rost, Robert W. Emery. Multicentric T Cell Lymphoma in a Dromedary Camel (Camelus dromedarius). Journal of Zoo and Wildlife Medicine. 2005;36(4):727–729.

18. Ibrahim A, Hussen J, Shawaf T, Al-Hizab FA, Kiupel M. Disseminated gamma-delta T-cell lymphoma in a dromedary camel. Veterinary Record Case Reports. 2023;n/a(n/a):e650.

19. Khoury JD, Solary E, Abla O, Akkari Y, Alaggio R, Apperley JF, Bejar R, Berti E, Busque L, Chan JKC, Chen W, Chen X, Chng WJ, Choi JK, Colmenero I, Coupland SE, Cross NCP, De Jong D, Elghetany MT, Takahashi E, Emile JF, Ferry J, Fogelstrand L, Fontenay M, Germing U, Gujral S, Haferlach T, Harrison C, Hodge JC, Hu S, Jansen JH, Kanagal-Shamanna R, Kantarjian HM, Kratz CP, Li XQ, Lim MS, Loeb K, Loghavi S, Marcogliese A, Meshinchi S, Michaels P, Naresh KN, Natkunam Y, Nejati R, Ott G, Padron E, Patel KP, Patkar N, Picarsic J, Platzbecker U, Roberts I, Schuh A, Sewell W, Siebert R, Tembhare P, Tyner J, Verstovsek S, Wang W, Wood B, Xiao W, Yeung C, Hochhaus A. The 5th edition of the World Health Organization Classification of Haematolymphoid Tumours: Myeloid and Histiocytic/Dendritic Neoplasms. Leukemia. 2022;36(7):1703-1719.

20. Raval SH, Joshi DV, Patel BJ, Patel JG, Bhatt NG. Histological and immunohistochemical characterisation of T-Cell Lymphoma in A Camel. J Camel Pract and Res. 2015;22(2):247–250.

21. Tageldin MH, al Sumry HS, Zakia AM, Fayza AO. Suspicion of a case of lymphocytic leukaemia in a camel (Camelus dromedarius) in Sultanate of Oman. Rev Elev Med Vet Pays Trop. 1994;47(2):157–158.

22. Twomey DF, Barlow AM, Hemsley S. Immunophenotyping of lymphosarcoma

in South American camelids on six British premises. Vet J. 2008;175(1):133–135.

23. Valli VE, Bienzle D, Meuten DJ. Tumors of the Hemolymphatic System. In: Tumors in Domestic Animals. 2016:203–321.

24. Valli VE, Myint MS, Barthel A, et al. Classification of Canine Malignant Lymphomas According to the World Health Organization Criteria. Veterinary Pathology. 2010;48(1):198-211.